Task-dependent energetic analysis of a 3 d.o.f. industrial manipulator

Paolo Boscariol[1] Lorenzo Scalera[2]
Alessandro Gasparetto[3]

[1]DTG, Università degli Studi di Padova, Vicenza, Italy
[2]Faculty of Science and Technology, Free University of Bozen-Bolzano
[1]DPIA, Università degli Studi di Udine

Abstract

In this paper a preliminary analysis of the energetic performance of an industrial manipulator is presented. In particular, the paper investigates the effects of the trajectory planning on the overall energy consumption of the manipulator in a pick & place task, focusing also on the location of the path within the workspace. An electro-mechanical model of the actuators and the inverse dynamic model of the robot have been developed and used to estimate the robot energy consumption when executing a basic motion task. Results are then collected into energy consumption maps, showing how the location of the task within the robot workspace affects the energetic performance of the robot.

1 Introduction

One of the most relevant challenge in modern robotics is the reduction of energy consumption, especially when high speed operations and high volumes of production are needed. In recent years, the increasing of energy costs and the growing of environment awareness have driven engineers and researchers to find new solutions for energy saving. In this context, a classification and analysis of different methods and techniques for enhancing the energy performances of industrial manipulators can be found in [1]. Possible approaches are the design of lightweight robots [2, 3, 4], the use of regenerative power storage systems [5], the exploitation of the manipulator natural dynamics [6, 7], the robot model selection [8], and the planning of energy efficient trajectories.

Examples of energy-efficient motion planning approaches can be found in [9], where both time-optimal and energy-optimal trajectories are investigated for pick-and-place motion with a 6 degree-of-freedom (d.o.f.) manipulator, and in [10], where an energy saving method for industrial machines using simple motion trajectories is presented. Furthermore, in [11], point-to-point trajectories based on standard primitives have been employed for the overall energy reduction of a typical 1 d.o.f. mechatronic system, whereas a trajectory planning approach for the energy saving in a redundant robotic cell has been adopted in [12]. Alternatively, energy efficiency can be improved by reducing the actuator effort thorough motion design, as performed for industrial robots in [13, 14].

This is a pre-print of the article: Boscariol P., Scalera L., Gasparetto A. (2020) Task-Dependent Energetic Analysis of a 3 d.o.f. Industrial Manipulator. In: Berns K., Görges D. (eds) Advances in Service and Industrial Robotics. RAAD 2019. Advances in Intelligent Systems and Computing, vol 980. Springer, Cham https://doi.org/10.1007/978-3-030-19648-6_19

In literature several performance measures have been investigated to estimate the behavior of industrial manipulators, either by using global or local measures. Referring to the latter category, in [15], the application and graphical visualization of different indexes are applied to a SCARA manipulator, whereas in [16] a task-dependent performance index has been introduced and adopted to optimize the location of a pick-and-place task for an industrial parallel robot. This studies have been motivated by the fact that local performance indexes can be useful for highlighting the relationship between the robot and the task definition, and in particular they often provide a guidelines in the choice of the areas of the workspace in which 'better' robot performance can be achieved [17]. Robot performance can be measured by performance indexes focusing on some measurement of dexterity, force or speed exertion capability, or manipulability, but currently there are, to the best of Authors' knowledge, no performance index that are focused strictly on energy consumption. With this final goal in mind, the aim of this paper is to provide a preliminary analysis of the energetic performance of a 3 d.o.f. SCARA manipulator. The effects of the path and trajectory planning on the overall energy consumption are evaluated for a specific task: a common pick-and-place operation, as performed in [18]. On the basis of an electro-mechanical model of the manipulator, the influence of the location of the task within the robot workspace, as well as of the choice of motion law, are evaluated. Simulation results provide, for each considered trajectory, energy consumption maps for the performance evaluation and the optimal robot positioning.

2 Dynamic and electro-mechanical model

The industrial manipulator under consideration in this work is a 3 d.o.f. SCARA robot, designed according to the common RRP architecture. The dynamic model of the robot can be written by attributing to each link its specific inertial properties. The dynamic equations of motion, which describe the joint torques $\boldsymbol{\tau_j}$ as a function of the joint variables $\boldsymbol{q} = [q_1, q_2, q_3]^T$, can be derived by using the Lagrangian formalism, leading to the usual formulation:

$$\boldsymbol{\tau_j} = \boldsymbol{M}(\boldsymbol{q})\ddot{\boldsymbol{q}} + \boldsymbol{C}(\boldsymbol{q}, \dot{\boldsymbol{q}}) + \boldsymbol{f}_v\,\dot{\boldsymbol{q}} + \boldsymbol{F}_c\,\mathrm{sign}(\dot{\boldsymbol{q}}) \tag{1}$$

in which $\boldsymbol{M}(\boldsymbol{q})$ is the mass matrix of the manipulator, matrix $\boldsymbol{C}(\boldsymbol{q}, \dot{\boldsymbol{q}})$ accounts for the centrifugal and Coriolis effects, $\boldsymbol{f}_v$ is the diagonal matrix of viscous friction coefficients, and $\boldsymbol{F}_c$ is the diagonal matrix of Coulomb friction forces. In order to derive the electro-mechanical model of the actuators of the robot, assuming that brushless motors are used as in [12, 19], the motor torques vector $\boldsymbol{\tau}_m$ is related to the motor armature current vector $\boldsymbol{I}(t)$ as:

$$\boldsymbol{\tau_m}(t) = \boldsymbol{k}_t\,\boldsymbol{I}(t) \tag{2}$$

where $\boldsymbol{k}_t$ is the diagonal matrix of the individual motor torque constants. The armature model can be then introduced to describe the voltage drop $\boldsymbol{V}(t)$ across the motors of all the joints of the manipulator:

$$\boldsymbol{V}(t) = \boldsymbol{R}\boldsymbol{I}(t) + \boldsymbol{k}_b\,\dot{\boldsymbol{q}}_m(t) \tag{3}$$

where matrices $\boldsymbol{R}$ and $\boldsymbol{k}_b$ include each individual motor winding resistance and the back-emf constants, respectively, while $\dot{\boldsymbol{q}}_m$ is the motor velocities vector.

This is a pre-print of the article: Boscariol P., Scalera L., Gasparetto A. (2020) Task-Dependent Energetic Analysis of a 3 d.o.f. Industrial Manipulator. In: Berns K., Görges D. (eds) Advances in Service and Industrial Robotics. RAAD 2019. Advances in Intelligent Systems and Computing, vol 980. Springer, Cham https://doi.org/10.1007/978-3-030-19648-6_19

Finally, the motors input energy E_{robot} required to perform a generic operation over the time interval $t \in [t_a, t_b]$ can be found by computing the time integral of the instantaneous electric power drawn by the robot, expressed by the voltage-current product:

$$E_{robot} = \int_{t_a}^{t_b} \boldsymbol{V}^T(t)\, \boldsymbol{I}(t)\, dt \tag{4}$$

Equation 4 represents the net energetic balance of the robot within the time frame $[t_a, t_b]$, so that is the energy is evaluated without making any distinction between positive and negative values of the voltage-current product. This feature is however not very realistic, since the vast majority of of industrial robots are equipped with non-regenerative motor drives and negative electric power is simply dissipated on a braking resistor. Accordingly, to avoid subtracting the energy dissipated on the braking resistor from the energy balance, the computation of the integral of Eq. 4 is limited to positive values of the current-voltage product.

3 Task-dependent energetic performance evaluation

The dynamic model introduced in section 2 is here used to analyze the impact of the choice of the task on the energetic performance of the robot. The analysis is limited to a basic but commonly performed task, i.e. the translation of the robot end-effector along a straight line, as performed in pick & place operation. Given a fixed execution time and a fixed total displacement, such a task can be performed in infinite ways, provided that the initial and final point of the trajectory are left free. Additionally, the design of the task gains an additional degree of freedom if the motion law is left free as well. Under this assumptions the path of the end-effector of the robot can be parametrized by two values: the real positive value d, which measures the distance, defined on the horizontal plane $\{X, Y\}$ between the base of the robot and the mid-point of the trajectory, and α, which measures the angular distance between the line described by the path and the line along which d is measured: a graphical reference is provided in Fig. 1.

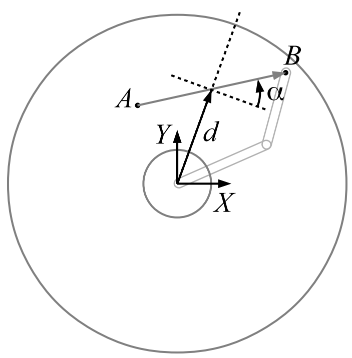

Figure 1: Parametrization of the path within the workspace of the robot

This is a pre-print of the article: Boscariol P., Scalera L., Gasparetto A. (2020) Task-Dependent Energetic Analysis of a 3 d.o.f. Industrial Manipulator. In: Berns K., Görges D. (eds) Advances in Service and Industrial Robotics. RAAD 2019. Advances in Intelligent Systems and Computing, vol 980. Springer, Cham https://doi.org/10.1007/978-3-030-19648-6_19

The base of the robot is set on the origin of the $\{X, Y\}$ reference frame, and the workspace of the robot is delimited by the two gray circles shown in Fig. 1. The task is represented by a vector that connects the starting point A with the final point B. Given the radial symmetry of the robotic configuration, all possible tasks are defined by values of d ranging from 0.1 m to 0.8 m, and for values of α between 0 and π radians. The kinematic and dynamic properties of the manipulator used for the computation of the energy costs are shown Table 1. The distance between point A and B is set, for all experiment, to be equal to 0.3 m and the total execution time is set to 0.5 s. The motion of the third axis of the robot is not included in the analysis, given that it is not influenced by the choice of the path. Referring to the motion profile, countless choices are available. Here four well-known options are taken into consideration: the trapezoidal speed profile, the harmonic speed profile, the third and fifth-degree polynomial profiles [20]. In all cases the motion design is performed in the operational space to ensure that the robot end-effector is moved along a straight line. For each of the four choices of the motion profile, a sequence

Table 1: Mechanical and electric parameters of the SCARA robot

Parameter	**Joint 1**	**Joint 2**	**Joint 3**
Link length	0.45 m	0.35 m	-
Link mass	14 kg	18 kg	2 kg
Gear ratio	1/80	1/50	1/30
Motor inertia	$3 \cdot 10^{-4}\ kgm^2$	$2 \cdot 10^{-4}\ kgm^2$	$1 \cdot 10^{-4}\ kgm^2$
Viscous friction coefficient	0.001 Nms/rad	0.001 Nms/rad	0.001 Nms/rad
Coulomb friction force	$2 \cdot 10^{-2}$ Nm	$2 \cdot 10^{-2}$ Nm	$2 \cdot 10^{-2}$ Nm
Motor winding resistance	3 Ω	3 Ω	3.5 Ω
Motor back-emf constant	0.6 Vs/rad	0.6 Vs/rad	0.6 Vs/rad
Motor torque constant	0.6 Nm/A	0.6 Nm/A	0.6 Nm/A

of trajectories are simulated and the resulting energy consumption data are collected and plotted in the energy maps shown in Fig. 2 and 3. Figure 2(a)

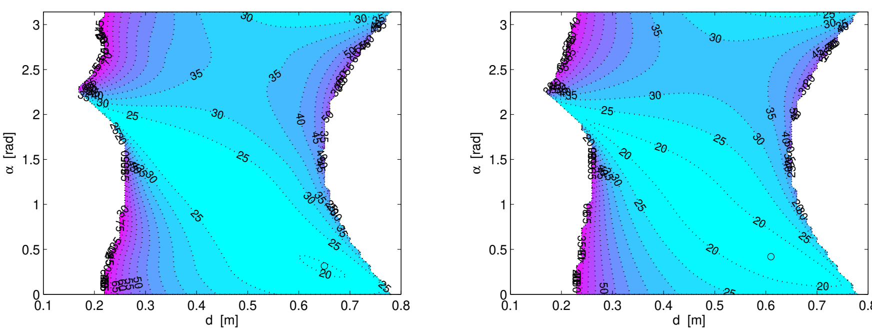

(a) (b)

Figure 2: Energy consumption maps: trapezoidal (a) and harmonic (b) motion profiles

shows a contour plot of the total energy delivered to the robot when moving

This is a pre-print of the article: Boscariol P., Scalera L., Gasparetto A. (2020) Task-Dependent Energetic Analysis of a 3 d.o.f. Industrial Manipulator. In: Berns K., Görges D. (eds) Advances in Service and Industrial Robotics. RAAD 2019. Advances in Intelligent Systems and Computing, vol 980. Springer, Cham https://doi.org/10.1007/978-3-030-19648-6_19

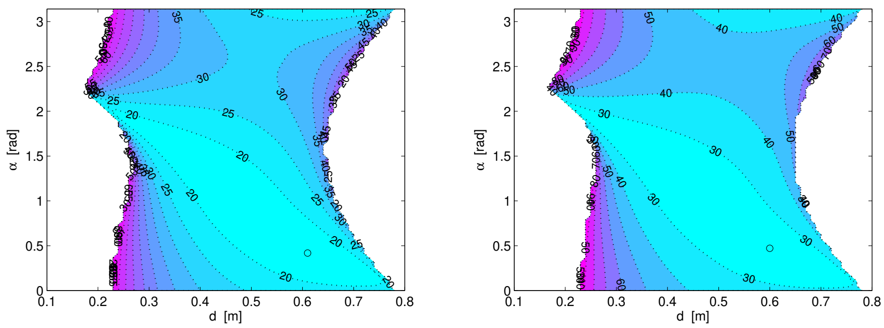

(a) (b)

Figure 3: Energy consumption maps: third order (a) and fifth order (b) polynomial motion profiles

according to a trapezoidal speed profile: each point corresponds to a specific choice of d and α and the the energy consumption is measured in Joules. Darker shades of purple represent the tasks associated with higher energy consumption, while the white areas represent tasks that are either unfeasible, due to workspace limitations, or that imply unreasonable energetic requirements. The analysis is then repeated by using the harmonic profile for computing the contour plot in Fig. 2(b), and then by using the third and fifth degree polynomial profiles for the energy maps in Fig. 3(a) and 3(b), respectively. All maps also include a small black circle, which identifies the minimum energy task: in all four cases the energetic optimality is found for values of d close to 0.6 m and for values of α in the neighborhood of 0.5 radians. According to the task parametrization, as it can be seen in Fig. 1, $\alpha = 0$ corresponds to 'rightwards' motion along the tangential direction, while $\alpha = \pi/2$ refers to an 'outward' motion along the radial direction. The analysis of the energy maps in Fig. 2 and 3 suggest that, as expected, the different motion profiles result in different energy consumptions, and that the best choice, among the one analyzed here, is the third degree polynomial function. Despite the relative differences between the absolute values of the energy consumption, all maps show a similar 'shapes', meaning that the higher energetic efficiency is found for similar values of d and α in all cases. It can be therefore inferred that the total energy consumption associated with a single task is affected by an higher degree by the task collocation within the workspace, rather than by the choice of the specific motion profile. In other words, in the case under consideration, as far as the energy consumption in concerned, the critical choice is the definition of the task position within the workspace.

All four maps show that the best choices for the definition of the task are found within and area whose shape resembles an 'hysteresis loop', and that generally higher efficiency is found when operating the robot towards the external areas of the workspace. The influence of the motion direction is more clearly understood by looking at Fig. 4: the red arrows represent the optimal displacements for 12 uniformly distributed distances from the base of the robot, and the blue arrow shows the overall optimal solution, which corresponds to the parameters $d = 0.61$ m and $\alpha = 0.4189$ rad. Each arrow connects point A and B, i.e.

This is a pre-print of the article: Boscariol P., Scalera L., Gasparetto A. (2020) Task-Dependent Energetic Analysis of a 3 d.o.f. Industrial Manipulator. In: Berns K., Görges D. (eds) Advances in Service and Industrial Robotics. RAAD 2019. Advances in Intelligent Systems and Computing, vol 980. Springer, Cham https://doi.org/10.1007/978-3-030-19648-6_19

the initial and final point of the trajectory, according to the parametrization shown in Fig. 1. All of them refer to the third degree motion profile, i.e. the less energetically expensive among the ones tested here. Figure 4 suggests that the radial motion is the best choice when working close to the robot base, and that a tangential motion is the best choice when operating towards the external boundaries of the workspace.

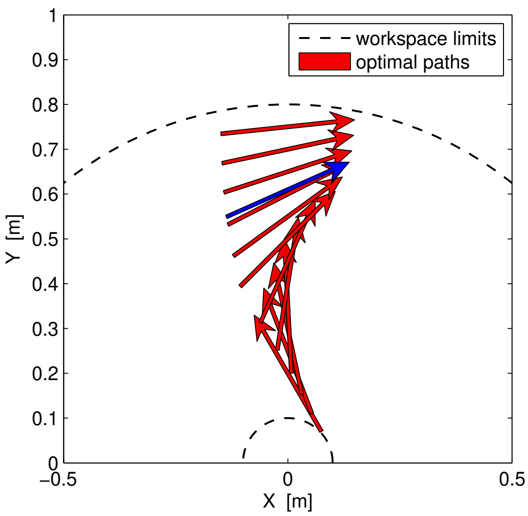

Figure 4: Optimal paths with varying distance from the base: optimal solution shown in red color

4 Conclusions

In this work a preliminary analysis of the energetic performance of a 3 d.o.f. industrial robot has been presented. The analysis focuses on the estimation of the energy consumption of the robot when executing a basic motion task, highlighting the influence of the choice of the motion profile and of the task positioning within the workspace. The numerical results indicate that the latter has a major impact on the energy consumption, and therefore the energy maps provided here can be used to define the optimal robot-workpiece relative positioning for improving the energy efficiency.

References

[1] G. Carabin, E. Wehrle, and R. Vidoni, "A review on energy-saving optimization methods for robotic and automatic systems," *Robotics*, vol. 6, no. 4, p. 39, 2017.

[2] P. Boscariol, P. Gallina, A. Gasparetto, M. Giovagnoni, L. Scalera, and R. Vidoni, "Evolution of a dynamic model for flexible multibody systems," in *Advances in Italian Mechanism Science*, pp. 533–541, Springer, 2017.

This is a pre-print of the article: Boscariol P., Scalera L., Gasparetto A. (2020) Task-Dependent Energetic Analysis of a 3 d.o.f. Industrial Manipulator. In: Berns K., Görges D. (eds) Advances in Service and Industrial Robotics. RAAD 2019. Advances in Intelligent Systems and Computing, vol 980. Springer, Cham https://doi.org/10.1007/978-3-030-19648-6_19

[3] R. Vidoni, A. Gasparetto, and L. Scalera, "3-D ERLS based dynamic formulation for flexible-link robots: theoretical and numerical comparison between the Finite Element Method and the Component Mode Synthesis approaches," *International Journal of Mechanics and Control*, 2018.

[4] R. Belotti, G. Caneva, I. Palomba, D. Richiedei, and A. Trevisani, "Model updating in flexible-link multibody systems," in *Journal of Physics: Conference Series*, vol. 744, p. 012073, IOP Publishing, 2016.

[5] K. Inoue, K. Ogata, and T. Kato, "An efficient induction motor drive method with a regenerative power storage system driven by an optimal torque," in *Power Electronics Specialists Conference, 2008. PESC 2008. IEEE*, pp. 359–364, IEEE, 2008.

[6] H. Goya, K. Matsusaka, M. Uemura, Y. Nishioka, and S. Kawamura, "Realization of high-energy efficient pick-and-place tasks of SCARA robots by resonance," in *Intelligent Robots and Systems (IROS), 2012 IEEE/RSJ International Conference on*, pp. 2730–2735, IEEE, 2012.

[7] G. Lu, S. Kawamura, and M. Uemura, "Proposal of an energy saving control method for SCARA robots," *Journal of Robotics and Mechatronics*, vol. 24, no. 1, pp. 115–122, 2012.

[8] M. Chemnitz, G. Schreck, and J. Krüger, "Analyzing energy consumption of industrial robots," in *Emerging Technologies & Factory Automation (ETFA), 2011 IEEE 16th Conference on*, pp. 1–4, IEEE, 2011.

[9] K. Paes, W. Dewulf, K. Vander Elst, K. Kellens, and P. Slaets, "Energy efficient trajectories for an industrial ABB robot," *Procedia Cirp*, vol. 15, pp. 105–110, 2014.

[10] P. M. Ho, N. Uchiyama, S. Sano, Y. Honda, A. Kato, and T. Yonezawa, "Simple motion trajectory generation for energy saving of industrial machines," *SICE Journal of Control, Measurement, and System Integration*, vol. 7, no. 1, pp. 29–34, 2014.

[11] G. Carabin, R. Vidoni, and E. Wehrle, "Energy saving in mechatronic systems through optimal point-to-point trajectory generation via standard primitives," in *Second Int. Conf. of IFToMM ITALY*, pp. 20–28, Springer, 2018.

[12] P. Boscariol and D. Richiedei, "Energy saving in redundant robotic cells: Optimal trajectory planning," in *IFToMM Symposium on Mechanism Design for Robotics*, pp. 268–275, Springer, 2018.

[13] Z. Shiller, "Time-energy optimal control of articulated systems with geometric path constraints," *Journal of dynamic systems, measurement, and control*, vol. 118, no. 1, pp. 139–143, 1996.

[14] G. Trigatti, P. Boscariol, L. Scalera, D. Pillan, and A. Gasparetto, "A new path-constrained trajectory planning strategy for spray painting robots," *The International Journal of Advanced Manufacturing Technology*, vol. 98, no. 9-12, pp. 2287–2296, 2018.

This is a pre-print of the article: Boscariol P., Scalera L., Gasparetto A. (2020) Task-Dependent Energetic Analysis of a 3 d.o.f. Industrial Manipulator. In: Berns K., Görges D. (eds) Advances in Service and Industrial Robotics. RAAD 2019. Advances in Intelligent Systems and Computing, vol 980. Springer, Cham https://doi.org/10.1007/978-3-030-19648-6_19

[15] T. Tanev and B. Stoyanov, "On the performance indexes for robot manipulators," *Problems of engineering cybernetics and robotics*, vol. 49, pp. 64–71, 2000.

[16] G. Boschetti, R. Rosa, and A. Trevisani, "Optimal robot positioning using task-dependent and direction-selective performance indexes: General definitions and application to a parallel robot," *Robotics and Computer-Integrated Manufacturing*, vol. 29, no. 2, pp. 431–443, 2013.

[17] S. Patel and T. Sobh, "Manipulator performance measures-a comprehensive literature survey," *Journal of Intelligent & Robotic Systems*, vol. 77, no. 3-4, pp. 547–570, 2015.

[18] G. Boschetti, "A picking strategy for circular conveyor tracking," *Journal of Intelligent & Robotic Systems*, vol. 81, no. 2, pp. 241–255, 2016.

[19] D. Richiedei and A. Trevisani, "Analytical computation of the energy-efficient optimal planning in rest-to-rest motion of constant inertia systems," *Mechatronics*, vol. 39, pp. 147–159, 2016.

[20] L. Biagiotti and C. Melchiorri, *Trajectory planning for automatic machines and robots.* Springer Science & Business Media, 2008.

This is a pre-print of the article: Boscariol P., Scalera L., Gasparetto A. (2020) Task-Dependent Energetic Analysis of a 3 d.o.f. Industrial Manipulator. In: Berns K., Görges D. (eds) Advances in Service and Industrial Robotics. RAAD 2019. Advances in Intelligent Systems and Computing, vol 980. Springer, Cham https://doi.org/10.1007/978-3-030-19648-6_19